DOI: 10.1002/ejic.200600621

Size- and Shape-Controlled Synthesis and Assembly of a Silver Nanocomplex in UV-Irradiated TSA Solution

Liangbao Yang,[a] Yuhua Shen,*[a] Anjian Xie,[a] Jianjun Liang,[b] Shikuo Li,[a] and Qingfeng Zhang[a]

Keywords: Nanostructures / Silver / Photochemistry / Self-assembly

In this paper we describe the size-controlled synthesis of a silver nanocomplex based on the reduction of silver nitrate ($AgNO_3$) by UV-irradiated tungstosilicate acid [$H_4(SiW_{12}O_{40})$, TSA] solution. This method allows the synthesis of ellipsoidal particles with an average size that is tunable between 2.4 and 84 nm by varying the molar ratio of silver nitrate to TSA, the pH of the reaction solution, and the reaction temperature. Silver nanorods can be formed from the ellipsoidal nanoparticles by controlling the aging time. The formation mechanism of these nanorods is also discussed. The nanoparticles are characterized by UV/Vis spectroscopy, FTIR spectroscopy, XRD analysis, XPS, electron diffraction (ED), TEM, and with a Zetasizer instrument.

Introduction

Metal nanoparticles are being investigated in considerable detail due to their exciting potential applications in catalysis,[1] biological and chemical sensing,[2,3] and optoelectronics.[4] One of the most important current challenges is to develop experimental recipes that would enable nanoparticle shape-control in addition to size and polydispersity. A number of nanoparticle morphologies such as wires,[5] rods,[6] cubes,[7] and nanotriangles/prisms[8] can now be routinely synthesized by different chemical methods.

Silver nanoparticles, in particular, are of great interest because of their ability to efficiently interact with light by virtue of plasmon resonances, which are the collective oscillations of the conduction electrons in the metal. Silver nanoparticles certainly have the potential to be the building blocks of future photonic and plasmonic devices as the field of nanotechnology matures.

A requirement for this progress is the development of a method that can reliably produce large quantities of silver nanoparticles with a controlled size distribution as different applications will require particles with various dimensions and the ability to tailor surface chemistry. The ideal method of synthesis should yield essentially naked particles so that different surface functionalities can be readily introduced for template-assisted or self-assembly based fabrication methods for nanoscale devices.

The use of tungstosilicate acid [$H_4(SiW_{12}O_{40})$, TSA] to synthesize silver nanoparticles is an important synthetic method. TSA ions form a subset of polyoxometalates of the Keggin structure. These polyoxometalates have the general formula $(XM_{12}O_{40})^{(8-n)-}$, where M is W or Mo and X is a heteroatom such as P, Si, or Ge, with n being the valency of X.[9] The TSA ions, accompanying cations, and other components such as water are arranged in a well-defined secondary three-dimensional structure, the stability of which depends on the nature of the counterions, the amount of water, etc.[10] It is well known that Keggin ions undergo stepwise multielectron redox processes without a structural change[11] and can be reduced electrolytically, photochemically, and chemically (with suitable reducing agents). They are a large category of metal oxygen cluster anions with well-defined structures and properties and have diverse applications in the fields of analytical chemistry, biochemistry, and solid state devices, and have been used as antiviral and antitumor reagents. Their redox chemistry is characterized by their ability to accept and release a certain number of electrons, in distinct steps, without decomposition.[12] Recently, Papaconstantinou and co-workers have shown that photochemically reduced polyoxometalates of the Keggin structure phosphotungstic acid $(PW_{12}O_{40})^{3-}$[13] lead to the formation of the corresponding metal nanoparticles. Sastry and co-workers have used $(PW_{12}O_{40})^{3-}$ ions for making phase-pure core–shell nanoparticles.[14] They have also used $(PW_{12}O_{40})^{3-}$ ions as a template for the in-situ growth of metal nanoparticles,[15,16] star-shaped calcium carbonate crystals,[17] and CdS nanoparticles.[18]

[a] School of Chemistry and Chemical Engineering, Anhui University,
Hefei 230039, P. R. China
E-mail: s_yuhua@163.com
Fax: +86-551-510-7342
[b] Chuzhou Vocational Technology College,
Chuzhou 239000, P. R. China

Supporting information for this article is available on the WWW under http://www.eurjic.org or from the author.

$(PW_{12}O_{40})^{3-}$ is stable at a pH of around 1, whereas TSA is stable up to a pH of about 5.[5] It should be noted that these two Keggin ions have a similar photochemical behavior except that the reaction rates with $(PW_{12}O_{40})^{3-}$ appear to be about two to three times faster than those with TSA.[19] This faster reaction rate often leads to difficulty in controlling the morphologies of the particles, therefore TSA is preferable. In this paper, a general synthetic method that produces silver nanoparticles in water is proposed. The method offers the advantages of being easily scalable and able to produce particles that exhibit long-term stability. The sizes of the synthesized particles can be varied from several to eighty nanometers simply by varying the reaction conditions such as the molar ratio of silver nitrate to TSA, the pH value of the reaction solution, or the reaction temperature. At the same time, silver nanorods can be obtained by varying the aging time. The role of the TSA in directing the morphology of the Ag-TSA colloidal particles for the growth of nanoparticles of a range of chemical compositions is an exciting aspect of the work with important future implications in nanoparticle design. Another area where applications of such composites could arise is in the area of catalysis. Combining the Keggin-ion scaffold with catalytically active metal nanoparticles, such as Rh or Pd, could lead to novel catalysts wherein the Keggin ion and metal components catalyze different reactions simultaneously.[16] To the best of our knowledge, this is the first time to study the size-controlled and shape-controlled synthesis of silver nanoparticles by the templates of TSA colloidal particles. The TSA template may be removed by simple dissolution in an alkaline medium leaving behind reasonably intact silver nanoparticle superstructures. Presented below are details of this investigation.

Results and Discussion

A representative Keggin structure $(SiW_{12}O_{40})^{4-}$ was chosen to study the reaction between $(SiW_{12}O_{40})^{5-}$ and Ag^+ ions. The $(SiW_{12}O_{40}]^{5-}$ ion was obtained by photolysis ($\lambda >$ 280 nm) of a deaerated 2-propanol/$(SiW_{12}O_{40})^{4-}$ aqueous solution, in the presence of, for instance, 2-propanol as a sacrificial reagent[20] [Equation (1)].

$$2(SiW_{12}O_{40})^{4-} + (CH_3)_2CHOH \rightarrow 2(SiW_{12}O_{40})^{5-} + (CH_3)_2C{=}O + 2H^+ \quad (1)$$

After UV irradiation, the above solution gradually turned from colorless to grey (Ag) [Equation (2)]. This should be due to two reasons: one is the ability of the reduced $(SiW_{12}O_{40})^{5-}$ to transfer the electrons efficiently to silver ions;[21] the other is the lower potential of the one-equivalent-reduced tungstate couple $(SiW_{12}O_{40})^{4-}$/$(SiW_{12}O_{40})^{5-}$ (0.057 V vs. NHE;) relative to Ag^+/Ag^0 (0.799 V vs. NHE).

$$(SiW_{12}O_{40})^{5-} + Ag^+ \rightarrow (SiW_{12}O_{40})^{4-} + Ag \quad (2)$$

Furthermore, TSA ions can be utilized cyclically as oxidizing agent or reducing agent according to Equations (1) and (2).

Figure 1 shows the UV/Vis spectra recorded for a mixture of 1 mM $AgNO_3$ and 1 mM TSA at different stages of treatment. Prior to UV irradiation, it can be seen that there is no absorption in the visible region (0 h, Figure 1A), whereas after UV irradiation absorption bands are observed in the region 460–478 nm with the reaction time ranging from 20 to 300 min. These absorption bands are characteristic of silver nanoparticles and are caused by excitation of surface-plasmon vibrations.[22] Figure 1B shows the changes of wavelength and absorbance with different reaction time. From Figure 1, we can see that the absorption band becomes sharper and the resonance intensity increases, both of which are due to the increase of the number of silver nanoparticles during the whole process. A gradual shift of surface plasmon band (from 460 to 478 nm) is commensurate with the increasing $(SiW_{12}O_{40})^{5-}$ mol fraction. It can be seen that all the peaks are located at positions between those for pure $(SiW_{12}O_{40})^{5-}$ and Ag nanoparticle plasmon bands (730 and 413 nm, respectively, as reported

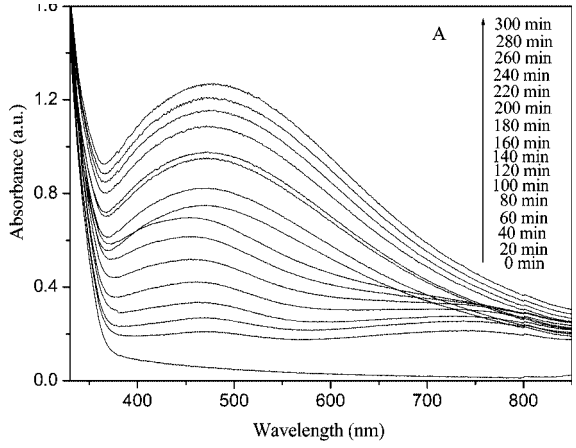

Figure 1. (A) UV/Vis spectra (330–850 nm) recorded for an aqueous mixture of 1 mM $AgNO_3$ and 1 mM TSA at different times of treatment. 0 h: before UV irradiation; 20–300 min: after UV irradiation. (B) Changes of wavelength and absorbance with reaction time. The inset shows one of the spectra of Figure 1A in the region from 210 to 330 nm.

earlier).[13,23,24] The presence of only one plasmon resonance, which shifts gradually from nanosilver to $(SiW_{12}O_{40})^{5-}$ ion particle plasmon bands clearly suggests the formation of TSA-silver nanocomposites rather than a segregated structure, as two bands would be observed in the latter case.[14] Thus, the UV-irradiated TSA ions reduce the Ag^+ ions, presumably on the surface of the TSA colloidal particles. It is notable that, in all experiments, the tungstosilicate acid structure remains intact in the process, as determined by the stability of the absorbance peak at 263 nm (shown in the inset of Figure 1B), which is characteristic of the oxidized form of TSA.[13]

In order to study the interaction between $AgNO_3$ and TSA during UV irradiation, the dynamic process of Ag-TSA colloid formation was analyzed by monitoring the conductance of a mixture consisting of equal volumes of 1 mM TSA and 1 mM $AgNO_3$ solutions (the conductance value of 1 mM aqueous TSA is 1.060 mS while that of 1 mM $AgNO_3$ is 0.532 mS). Figure 2 shows the conductance of the Ag-TSA reaction mixture measured as a function of the reaction time. After $AgNO_3$ is added to the TSA solution, it can be seen that the conductivity increases slowly. The reason for this is that the silver cations react with TSA anions to form a strong electrostatic complexation in solution. During complexation of silver ions with TSA anions, it is expected that the mobility of ions in solution would decrease, although the concentration of the ions increases swiftly. As UV irradiation progresses, the silver ions are reduced. At the end of the reaction the silver ions have been reduced completely, complexation of the silver cations and TSA anions in solution disappears, and plenty of TSA anions are generated. This means that the solution conductivity increases steadily and saturates after about 5 h of reaction, which is therefore an estimate of the optimum reaction time for the formation of this colloidal Ag nanocomplex.

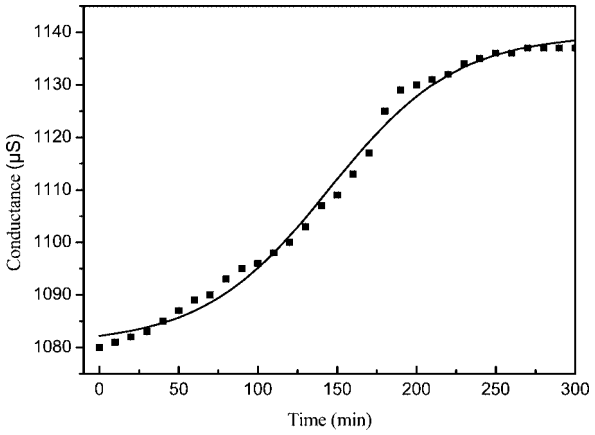

Figure 2. Conductivity measured as a function of time after mixing equal-volume aqueous solutions of 1 mM TSA and 1 mM $AgNO_3$ and irradiating for 5 h.

The XRD pattern recorded from a drop-coated film of the UV-irradiated sample on a glass substrate is shown in Figure 3. The (111), (200), (220), and (311) Bragg reflections of face-centered cubic (fcc) silver are clearly observed. Some of the Bragg reflections corresponding to the TSA structure (indicated by an asterisk) indicate that the formation of silver nanoparticles on the Ag^+-TSA colloidal particle template does not disrupt the basic structure of TSA. The XRD pattern recorded from a drop-coated film of the Ag-TSA nanocomplex solution after alkali dissolution of the TSA scaffold is shown as curve b in Figure 3. It is clear that the Bragg reflections of the TSA scaffold have disappeared, leaving behind just the Bragg reflections of the Ag nanoparticle assembly.

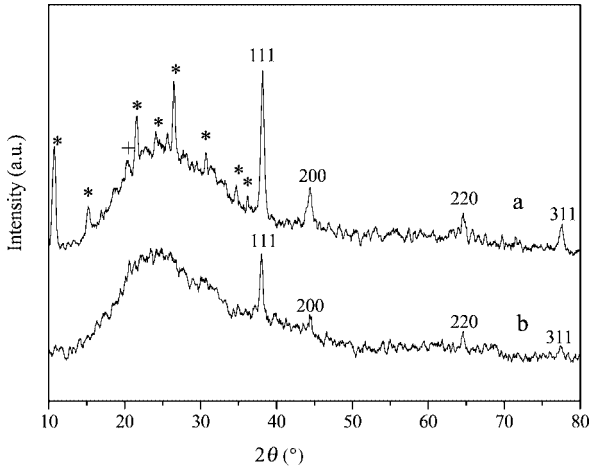

Figure 3. XRD patterns recorded from drop-coated films on glass substrates of silver nanoparticles synthesized by reaction of UV-irradiated TSA solution with aqueous $AgNO_3$ before (curve a) and after base treatment (curve b). The Bragg reflections marked * correspond to TSA.

Figure 4 shows the XPS W_{4f} and Ag_{3d} core-level spectra recorded from drop-coated films of the Ag-TSA solution on a Si (111) substrate. Figure 4A shows the W_{4f} spectrum recorded from the Ag-TSA film. This spectrum can be resolved into spin-orbit pairs (splitting $\approx$ 2.15 eV) with a $4f_{7/2}$ binding energy (BE) of 35.19 eV (curve 1 in Figure 4A). Figure 4B shows the Ag_{3d} core-level spectrum. The Ag_{3d} spectrum resolves into two spin-orbit components. The Ag $3d_{5/2}$ and $3d_{3/2}$ peaks occur at a BE of 367.8 and 373.8 eV, respectively, and correspond to metallic silver.[25] The result demonstrates that only one form of Ag is present in solution, in the form of Ag^0. There is no evidence for additional components in the Ag_{3d} spectrum, which indicates the complete reduction of the Ag^+ ions in the UV-irradiated TSA solution.

Figure 5A–D show representative TEM images recorded from a drop-coated film of the Ag-TSA solution after aging for 1, 6, 24, and 48 h, respectively. Figure 5A clearly show that there are only densely populated ellipsoidal or irregular structures. The crystalline nature of the silver nanoparticles forming the ellipsoidal or irregular crystal is revealed by the typical electron diffraction pattern shown in the inset of Figure 5A. The four fringe patterns observed, with spacings of 2.360, 2.021, 1.408, and 1.230 Å, are consistent with the fcc polycrystalline silver (111), (200), (220), and (311) spacings of 2.359, 2.044, 1.445, and 1.231 Å. Figure 5D shows

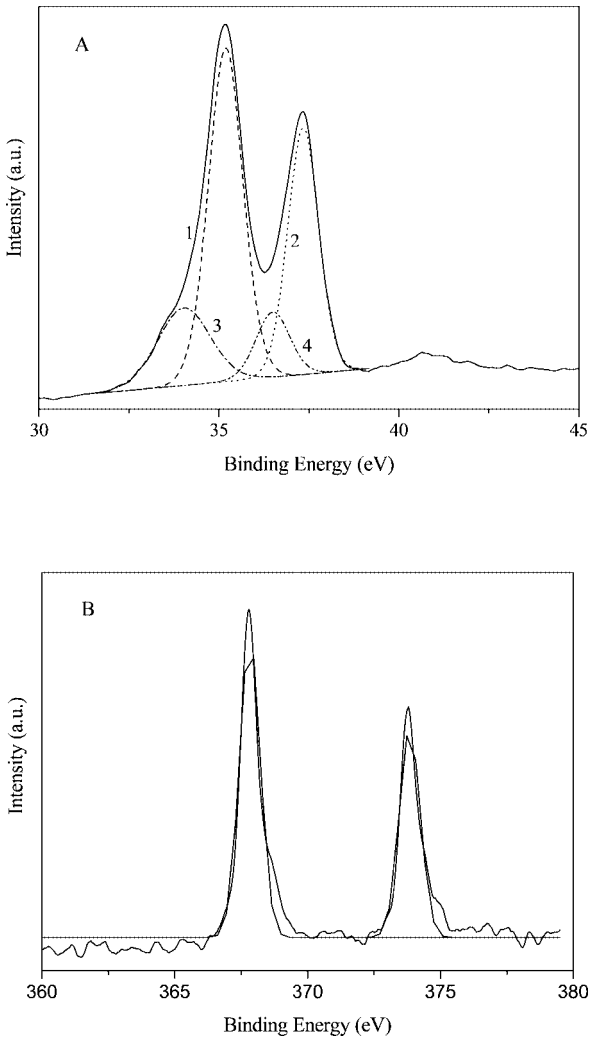

Figure 4. XPS recorded from drop-coated films of the Ag-TSA solution on a Si(111) substrate. (A) W 4f core-level spectrum together with two spin-orbit pairs (1, 2 and 3, 4). (B) Ag 3d core-level spectrum.

a representative TEM image recorded from a drop-coated film of the silver-nanocomplex solution after aging for 48 h. The surface of the rods is smooth and their structure is well-defined, with an average length and diameter of 1250 and 80 nm, respectively (a particle-size-distribution measurement was made from 140 nanorods). The aspect ratio (AR) of the silver nanorods in Figure 5D is estimated to be 13.2 ± 5.0. From the TEM image, it can be seen that the nanorods are smooth. In addition to the rod-shaped silver crystals, a lot of irregular crystals are also observed at the bottom left-hand corner of the image (Figure 5D), which implies that the nanorods possibly develop from the original irregular crystals.

The crystallinity of the nanorods was further studied by electron diffraction. As can be seen in the inset of Figure 5D, the ED patterns demonstrate the highly crystalline nature of the particles. From the electron diffraction analysis, the reflection assignments agree well with the results of nanowires reported previously,[26–28] thus demonstrating

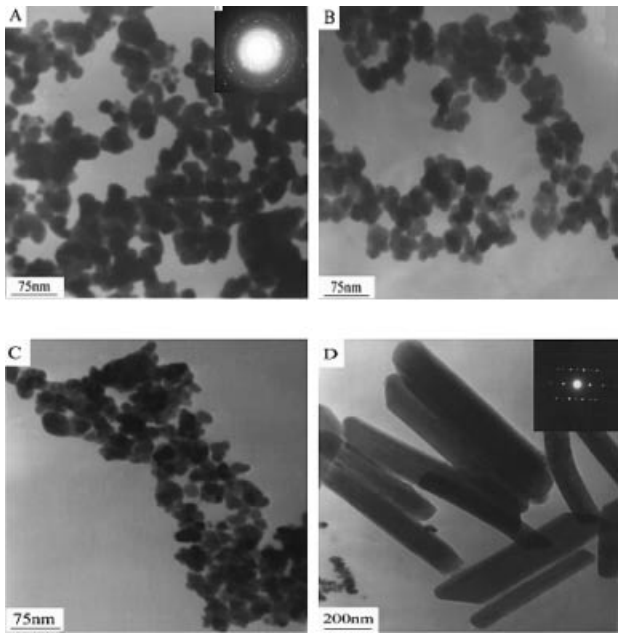

Figure 5. Representative TEM images of Ag nanocrystals obtained at different aging times after reaction (A–D). The insets in A and D are the electron diffraction patterns.

that the rod is formed by a cyclic penta-tetrahedral twin crystal in which five {111} twin boundaries are arranged radially to the [110] direction of the elongation axis. The rod has a pentagonal cross-section and is bound by five {100} side faces and five {111} faces at each end. In accordance with this structure feature, the rod should grow through the decahedral twinned particles with a diameter similar to the transverse length of the rods. The longitudinal and transverse lengths of the rods normally increase in the cases of smaller amounts of seeds. The rod formation possibly occurs in the early aggregation step of the initial particles.

It has been noticed that this kind of reaction takes place within a few seconds.[16] A lot of silver is generated in the first few seconds, so silver "seeds" can be formed, although no silver nanorods are generated at this stage. However, this in itself is not enough to form silver nanorods from silver seeds. Nanorod nucleation is thought to require twinned seed particles, so seed aggregation as a source of twinning may be an important step of nanorod synthesis.[29] On the other hand, the distance between two silver seeds is short, therefore some silver monomers can easily move and adsorb onto the deposited seeds and these aggregated seeds can form nanorods by subsequent recrystallization. So, we think that the growth mode for nanorods in our work is a type of seed-mediated growth mechanism.[29–31]

To understand the formation of large silver nanorod assemblies better, the kinetics of crystallization were monitored as a function of aging time. After aging for 1 h, ellipsoidal or irregular-shaped particles were obtained (Figure 5A). After aging for 6 h the long, irregular crystals begin to take shape and the number of ellipsoidal crystals decreases (Figure 5B). This is the initial stage of silver nano-

rod formation from ellipsoidal silver particle seeds. After aging for 24 h (Figure 5C) the Ag nanorods have almost formed, and when the aging time is prolonged to 48 h the silver nanorods grow into a well-organized shape (Figure 5D). The silver cubes are stable when they are separated from solvents. We found that the dry silver cubes do not change at all after being kept in air for several months.

To discount the possibility of UV-irradiated 2-propanol being the reducing agent for silver ions and thus for nanoparticle formation, a control experiment was performed in which 2 mL of 2-propanol was added to 20 mL of a 1 mM aqueous, deaerated solution of $AgNO_3$ and irradiated for 5 h. There was no change in color of the $AgNO_3$ solution after UV irradiation, which indicates that the product of UV-irradiated 2-propanol is not responsible for the reduction of $AgNO_3$. In the UV/Vis spectrum, the characteristic silver absorption band cannot be observed (see UV/Vis spectrum in Figure S1 in the Supporting Information).

Figure 6 shows the dependence of the particle diameter on the different molar ratios of Ag^+ ion to TSA. Parts A–D of Figure 6 show four samples of Ag-TSA nanoparticles corresponding to 1:10, 1:4, 1:2, and 2:1 molar ratios, respectively. These samples have mean diameters of 2.4, 22, 38, and 75.3 nm, respectively. As demonstrated in Figure 6, the size of these Ag-TSA nanoparticles can be conveniently controlled simply by varying the molar ratio, which changes from 0.1 to 2. The diameter increases monotonically from about 2.4 to about 75.3 nm. However, the growth rate decreases gradually, and when the molar ratio is above 2 there is only a small increase in the diameter of the silver nanoparticles. We also noticed that the color reflects the nanoparticle size in our experiments. By following the evolution of the color changes, we observed that a black color represents a colloidal size of about 70 nm and that the suspension of 10-nm-diameter Ag-TSA nanoparticles has, in fact, a grayish appearance, although it appears at lower concentrations. These changes may be directly related to the absorption features of the particles in the visible region of the spectra. It is not unusual that the size of the particles increases as a result of decreasing the relative concentrations of the reducing agent. This behavior is similar to that found in many chemical reduction approaches to nanosystems because the nucleation and growth sequences are both affected by the relative concentrations of the reducing agent and the precursor.[32] In our case, we think that the nucleation process is overwhelmingly faster than particle growth at the higher relative concentrations of the reducing agent, which results in smaller sized particles.

Figure 7 shows the dependence of the Ag-TSA nanoparticles' diameter on the pH of the solution. Parts A–D of Figure 8 show four samples of Ag-TSA nanoparticles corresponding to pH 1, 2, 3, and 4, respectively. The mean diameters of these four samples are 82, 22.8, 5.7, and 2.8 nm, respectively. Figure 7 clearly shows that the diameter decreases continuously with an increase in pH from 1 to 4. However, the rate of decrease diminishes gradually, and when the pH is near 4 there is only a small decrease in the diameter of the nanoparticles. The variation of pH does not

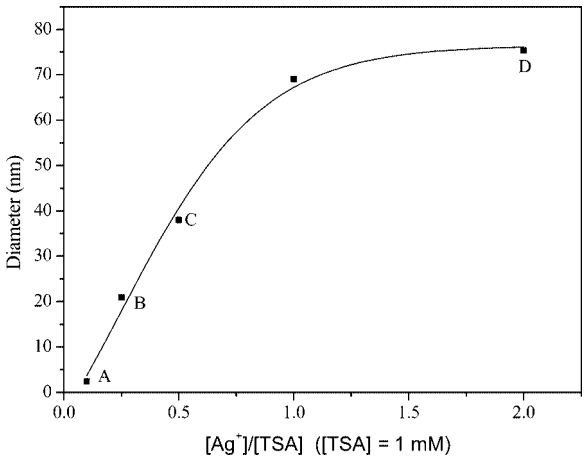

Figure 6. Dependence of the Ag-TSA nanoparticle diameter on the different molar ratio of Ag^+ ion to TSA. A–D show four samples of Ag-TSA nanoparticles corresponding to 1:10, 1:4, 1:2, and 2:1 molar ratios (T = 20 °C; [Ag^+] = 1 mM; reaction time: 5 h; aging time: 1 h).

alter the rate of metal ions' recovery during the reaction.[33] In other words, varying the pH does not alter the redox power of TSA, so the influence of pH on the particle diameter has nothing to do with this. We suppose that an electrostatic interaction leads to the dependence of the particle diameter on pH. Thus, with a decrease in pH the electrostatic interaction between the silver cations and TSA anions in solution becomes weaker, which allows the size of the particles to increase.

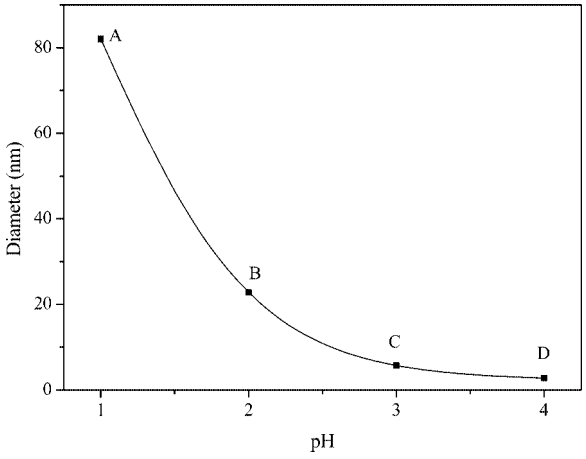

Figure 7. Dependence of the Ag-TSA nanoparticle diameters on pH. A–D show four samples of Ag-TSA nanoparticles with different diameters obtained at pH 1, 2, 3, and 4, respectively (T = 20 °C; [TSA] = 1 mM; [Ag+] = 1 mM; reaction time: 5 h; aging time: 1 h).

The dependence of the diameter of the Ag-TSA nanoparticles on temperature was also studied, as shown in Figure 8. Parts A–D of Figure 8 show four samples of Ag-TSA nanoparticles with different diameters obtained at 20, 40, 60, and 80 °C, respectively. The mean diameters of these four samples are 38, 7.6, 3.4, and 2.7 nm. As demonstrated in Figure 8, the size of these colloids can be conveniently controlled by simply varying the temperature. That is, the

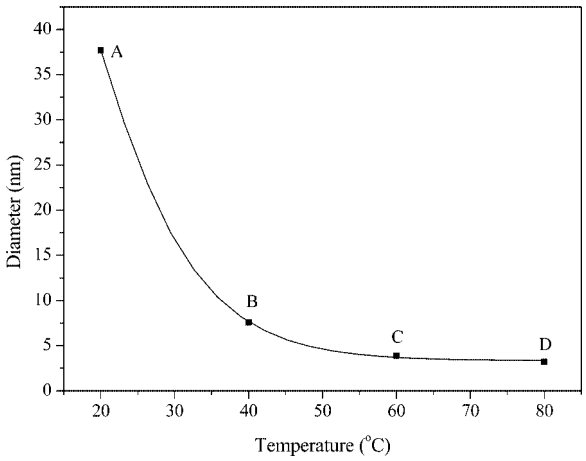

Figure 8. Dependence of the Ag-TSA nanoparticle diameters on reaction temperature. A–D show four samples of Ag-TSA nanoparticles with different diameters obtained at 20, 40, 60,and 80 °C, respectively.

diameter undergoes a continuous decrease with increasing temperature. However, the decrease rate diminishes gradually, and at 80 °C only a small decrease of the diameter of the particles is observed. With increasing temperature the silver ions have higher energies, which are larger than the affinity between TSA ions and silver ions, therefore these silver ions can move anywhere in the solution. That is to say, with an increase of temperature the rate of nucleation of silver nanoparticles accelerates, therefore the nucleation process is faster than the particle growth under these conditions and the size of the particles decreases.

To sum up, since the size of these Ag-TSA nanoparticle colloids can be conveniently controlled by simply varying the molar ratio of silver nitrate to TSA, the pH of the reaction solution, or the reaction temperature, the procedure described here should provide an effective route to ellipsoidal nanoparticles of Ag with controllable size. In principle, this procedure can be extended to several other noble metals that have been prepared as nanoparticles by reduction with TSA.

Conclusions

In conclusion, a facile method has been proposed to synthesize size-controlled silver nanocomplexes. The size of the nanoparticles can be controlled by varying the reaction conditions, and nanorods of silver can be formed by prolonging the aging time. The rods are found to generate through aggregation to form decahedral seeds followed by elongation along the [110] direction. The possibility of using the TSA framework as a UV-switchable reducing matrix is exciting and may be extended to the creation of other highly organized hybrid inorganic structures with possible applications in nanomaterials.

Experimental Section

Materials: $H_4(SiW_{12}O_{40})$ (TSA), $AgNO_3$, and 2-propanol were all obtained as A.R. grade from Shanghai Reagent Co. All other reagents were used as received.

Synthesis of the Silver Nanocomplex: In a typical experiment, 2-propanol (2 mL) and an aqueous deaerated solution of $AgNO_3$ (20 mL, 1 mM) were added to an aqueous deaerated solution of TSA (20 mL) under continuous stirring for 10 min and then allowed to age for 30 min. This mixture was irradiated with UV light (Pyrex filter, >280 nm, 450 W Hanovia medium pressure lamp) for 5 h. The solution changed to gray gradually, thus indicating the formation of silver nanoparticles. The corresponding control experiments under different reaction conditions, such as molar ratio of silver nitrate to TSA, pH of the reaction solution, and reaction temperature are similar to the above experiments.

To discount the possibility of UV-irradiated 2-propanol being the reducing agent for silver ions, and thus for nanoparticle formation, a control experiment was performed in which 2 mL of 2-propanol was added to 20 mL of a 1 mM aqueous deaerated solution of $AgNO_3$ and irradiated for 5 h.

Sample Characterization: UV/Vis spectroscopy measurements of the Ag-TSA solution at different stages of treatment were carried out with a TU-1901 model UV/Vis double beam spectrophotometer (Beijing Purkinje General Instrument Co., Ltd, China) operating at a resolution of 2 nm. XPS measurements of the silver nanoparticles synthesized by reduction of Ag^+ ions in a UV-irradiated TSA solution were carried out with a VG ESCALAB MKII instrument at a pressure greater than 10^{-6} Pa. The general scan and Ag 3d and W 4f core-level spectra were recorded with non-monochromated Mg-K_α radiation (photon energy = 1253.6 eV). The core-level binding energies (BEs) were aligned with respect to the C 1s binding energy (BE) of 285 eV. Samples for TEM analysis were prepared by drop-coating films of the Ag-TSA solution at different stages of reaction on carbon-coated copper TEM grids, allowing the grid to stand for 2 min, and then removing the excess solution with blotting paper. TEM measurements were performed with a JEM model 100SX electron microscope instrument (Japan Electron Co.) at an accelerating voltage of 80 kV. Selected-area electron diffraction measurements of the Ag nanoparticles were also carried out. XRD analysis of drop-coated films of the Ag-TSA solution on glass substrates was carried out with a MAP18AHF instrument (Japan MAC Science Co.). Conductance measurements were carried out to characterize the interaction between Ag^+ ions and TSA. The conductance of a mixture consisting of equal volumes of 1 mM TSA and 1 mM silver nitrate solutions was investigated. The conductivity of this solution as a function of reaction time was measured with a DDSJ-308A model conductivity meter (Shanghai Precision & Scientific Instrument Co., Ltd). The size distributions of nanoparticles were measured by PCS on a Zetasizer $3000HS_A$ instrument (Malvern Instruments Limited) at different molar ratios of silver nitrate to TSA, pH of the reaction solution, and reaction temperature.

Supporting Information (see footnote on the first page of this article): UV/Vis spectrum of a mixture of 2 mL 2-propanol and 20 mL of a 1 mM aqueous, deaerated solution of $AgNO_3$ after irradiation for 5 h.

Acknowledgments

This work was supported by the National Science Foundation of China (20471001, 20371001), the Specific Project for Talents of Science and Technology of the Universities of Anhui Province (2005hbz03), the Key Laboratory of Environment-Friendly Polymer Materials of Anhui Province, and the Science Foundation of Anhui Province (2006KJ155B).

[1] S. Mandal, D. Roy, R. V. Chaudhari, M. Sastry, *Chem. Mater.* **2004**, *16*, 3714–3724.
[2] T. A. Taton, C. A. Mirkin, R. L. Letsinger, *Science* **2000**, *289*, 1757–1760.
[3] N. Krasteva, I. Besnard, B. Guse, R. E. Bauer, K. Mullen, A. Yasuda, T. Vossmeyer, *Nano Lett.* **2002**, *2*, 551–555.
[4] M. L. Brongersma, J. W. Hartman, H. A. Atwater, *Phys. Rev. B* **2000**, *62*, 356–359.
[5] K. K. Caswell, C. M. Bender, C. J. Murphy, *Nano Lett.* **2003**, *3*, 667–669.
[6] F. Kim, J. H. Song, P. Yang, *J. Am. Chem. Soc.* **2002**, *124*, 14316–14317.
[7] Y. Sun, Y. Xia, *Science* **2002**, *298*, 2176.
[8] a) R. Jin, Y. Cao, C. A. Mirkin, K. L. Kelly, G. C. Schatz, J. G. Zheng, *Science* **2001**, *294*, 1901–1903; b) S. S. Shankar, A. Rai, B. Ankamwar, A. Singh, A. Ahmad, M. Sastry, *Nat. Mater.* **2004**, *3*, 482–488.
[9] J. A. Huheey, *Inorganic Chemistry*, 3rd ed., Harper and Row, New York, **1983**, p. 698.
[10] M. Misono, *Mater. Chem. Phys.* **1987**, *17*, 103–108.
[11] a) M. T. Pope, A. Muller, *Angew. Chem. Int. Ed. Engl.* **1991**, *30*, 34–48; b) V. Kogan, Z. Izenshtat, R. Neumann, *Angew. Chem. Int. Ed.* **1999**, *38*, 3331–3334.
[12] M. T. Pope in *Inorganic Chemistry Concepts*, Springer Verlag, West Berlin, **1983**, vol. 8, p. 101.
[13] A. Troupis, A. Hiskia, E. Papaconstantinou, *Angew. Chem. Int. Ed.* **2002**, *41*, 1911–1914.
[14] S. Mandal, P. R. Selvakannan, R. Pasricha, M. Sastry, *J. Am. Chem. Soc.* **2003**, *125*, 8440–8441.
[15] S. Mandal, D. Rautaray, M. Sastry, *J. Mater. Chem.* **2003**, *13*, 3002–3005.
[16] A. Sanyal, S. Mandal, M. Sastry, *Adv. Funct. Mater.* **2005**, *15*, 273–280.
[17] D. Rautaray, S. R. Sainkar, M. Sastry, *Langmuir* **2003**, *19*, 10095–10099.
[18] S. Mandal, D. Rautaray, A. Sanyal, M. Sastry, *J. Phys. Chem. B* **2004**, *108*, 7126–7131.
[19] A. Hiskia, A. Troupis, A. Hiskia, E. Papaconstantinou, *Environ. Sci. Technol.* **2001**, *35*, 2358–2364.
[20] a) E. Papaconstantinou, *Chem. Soc. Rev.* **1989**, *16*, 1–31; b) A. Hiskia, A. Mylonas, E. Papaconstantinou, *Chem. Soc. Rev.* **2001**, *30*, 62–69; c) A. Mylonas, A. Hiskia, E. Androulaki, D. Dimotikali, E. Papaconstantinou, *Phys. Chem. Chem. Phys.* **1999**, *1*, 437–440.
[21] I. A. Weinstock, *Chem. Rev.* **1998**, *98*, 113–170.
[22] S. Link, Z. I. Wang, M. A. El-Sayed, *J. Phys. Chem. B* **1999**, *103*, 3529–3533.
[23] P. Mukherjee, S. Senapati, D. Mandal, A. Ahmad, M. I. Khan, R. Kumar, M. Sastry, *ChemBioChem* **2002**, *3*, 461–463.
[24] A. Ahmad, P. Mukherjee, S. Senapati, D. Mandal, M. I. Khan, R. Kumar, M. Sastry, *Colloids Surf. B* **2003**, *28*, 313–318.
[25] C. S. Fadley, D. A. Shirley, *J. Res. Natl. Bur. Stand.* **1970**, *74A*, 543.
[26] a) Y. Sun, B. Mayers, T. Herricks, Y. Xia, *Nano Lett.* **2003**, *3*, 955–960; b) H. Hofmeister, S. A. Nepijko, D. N. Ievlev, W. Schulze, G. Ertl, *J. Cryst. Growth* **2002**, *234*, 773–781.
[27] C. J. Johnson, E. Dujardin, S. A. Davis, C. J. Murphy, S. Mann, *J. Mater. Chem.* **2002**, *12*, 1765–1770.
[28] I. Lisiecki, A. Filankembo, H. Sack-Kongehl, K. Weiss, M. P. Pileni, *J. Phys. Rev. B* **2000**, *61*, 4968–4974.
[29] H. Liao, J. H. Hafner, *J. Phys. Chem. B* **2004**, *108*, 19276–19280.
[30] a) Z. Wei, A. J. Mieszawska, F. P. Zamborini, *Langmuir* **2004**, *20*, 4322–4326; b) Z. Wei, F. P. Zamborini, *Langmuir* **2004**, *20*, 11301–11304.
[31] N. Taub, O. Krichevski, G. Markovich, *J. Phys. Chem. B* **2003**, *107*, 11579–11582.
[32] Z. H. Lin, C. R. Chris Wang, *Mater. Chem. Phys.* **2005**, *92*, 591–594.
[33] A. Troupis, A. Hiskia, E. Papaconstantinou, *Environ. Sci. Technol.* **2002**, *36*, 5355–5362.

Received: July 2, 2006
Published Online: September 20, 2006

